This is a postprint version of the following published document:

Monge, M., Adeva, P., Muñoz, A. & Pérez, P. (2019). Oxidation behaviour of tungsten with vanadium additions. *Fusion Engineering and Design*, vol. 146, pp. 783–786.

Oxidation behaviour of tungsten with vanadium additions

M.A. Monge[a],[*], P. Adeva[b], A. Muñoz[a], P. Pérez[b]

[a] Universidad Carlos III de Madrid, Dpto. de Física, Avda. de la Universidad 30, Leganés, 28911, Spain
[b] Centro Nacional de Investigaciones Metalúrgicas, Dpto. de Metalurgia Física, Avd. Gregorio del Amo 8, Madrid, 28040, Spain

ARTICLE INFO

ABSTRACT

The effect of vanadium additions on the oxidation behaviour of tungsten has been evaluated at 600 °C in dry air. Mass gain in V-containing tungsten alloys is practically the same than that of pure tungsten processed by a conventional route. The advantage of vanadium alloying arises from the suppression of periodical microcracking described during the oxidation of pure tungsten, although the scale developed during the initial stages is very porous and it is not an effective barrier for inward oxygen ingress. Further protection is conferred when an outermost dense WO_3 layer is formed at the air/scale interface by condensation of volatile W and V oxides, turning the kinetics from linear to parabolic.

1. Introduction

One of the toughest challenges for the successful development of the fusion reactors is the design and selection of the materials for the plasma-facing components (PFCs), especially for the divertor which must sustain the highest energy flux. Tungsten has been selected as the armour material for ITER (International Termonuclear Experimental Reactor). ITER main objective is to demonstrate the feasibility of the fusion energy as a source of secure and clean energy and it would drive to the construction of a demonstration fusion power plant (DEMO). Design requirements for DEMO are more extreme and demanding, compared to ITER, and a large effort has been focused on the assessment of safety issues associated with a nuclear power plant [1,2].

Although tungsten presents unique advantages that turn alloys based on this metal as the most appropriate plasma facing material (PFM), pure tungsten or any other currently developed PFM cannot withstand the extreme operating conditions of DEMO, such as fast neutron irradiation and very high energy loads [3]. Furthermore, PFCs based on pure tungsten pose a security risk in case of a loss-of-coolant accident (LOCA) and air ingress in the vacuum reactor vessel. In this scenario, the temperature of the PFCs could raise up to 1200 °C due to the nuclear decay heat in the absence of cooling, giving rise to the rapid oxidation of any tungsten component and formation of highly volatile radioactive oxides [2,4]. This would severely damage the reactor vessel and generate a radioactive cloud difficult to control. The

studies estimate rates of 10-100 kg h^{-1} of sublimated material for a fusion reactor with a full-tungsten armoured divertor.

Extensive studies have been devoted to develop new reduced activation tungsten base materials with improved mechanical properties and increased DBTT (Ductile-to-Brittle Transition Temperature) [5]. Previous results have shown that the W-V alloys present a significant increase in the strength and fracture toughness compared to pure tungsten or other reduced activation tungsten based materials such as W-Ti alloys and W reinforced with a dispersion of nanoparticles (Y_2O_3, La_2O_3 or TiC) [6–9]. This result is especially promising considering it has been obtained for the alloy in the as-produced state after HIP sintering and a thermal stress relieve treatment, which gives room for further improvement of the properties after adequate thermo-mechanical treatments. However, there is little information about the oxidation W-V alloys due to the complexity of oxidation kinetics and the wide variety of oxides that could be formed [10]. It has been reported that vanadium additions below 5 wt.% increase the oxidation resistance of W at high temperatures in coarse grained fully recrystallized W-V alloys produced following a different route [11] for exposures times up to 6 h.

This work studies the oxidation resistance and kinetics of the W-xV ($x = 2$, 4 wt.%) alloy and compares it with the behaviour of ITER-reference tungsten grade prepared by a conventional route. The study tries to establish if W-V alloys can mitigate the safety risk associated with the use of pure tungsten as PFM.

[*] Corresponding author.
Email address: mmonge@fis.uc3m.es (M.A. Monge).

2. Experimental procedure

W-xV (x = 2, 4 wt.%) alloys and a pure tungsten ingot (named as PM-W) were obtained through a powder metallurgical route process that include blending, mechanical alloying/grinding and subsequent HIP (see reference [12] for a detailed description). The initial elemental powders were 99.95% pure W and 99.5% pure V. For reference, samples from a rod of a swaged ITER-reference tungsten grade, 99.97% purity, (named as CP-W) were prepared [13]. The ingots were subjected to stress relief heat treatment at 1200 °C in vacuum for 2 h.

As reported in our previous researches [6,12,14], the microstructure of W-xV (x = 2, 4 wt.%) alloys presents a bimodal grain size distribution embedding a homogeneous distribution of irregularly shaped pools of vanadium".

Coupons of $10 \times 10 \times 1$ mm^3 were used for oxidation tests at 600 °C in air. All major surfaces were abraded on successively finer silicon carbide papers, then mechanically polished with a 0.3 alumina suspension and cleaned with ethanol. Mass gain curves were monitored continuously during isothermal thermogravimetric tests for exposures up to 100 h. A continuous flow of dry air (dewpoint below −40 °C) was produced using an air compressor. Oxidation kinetics were evaluated by fitting mass gain curves to a power law equation of the form $\Delta W = kt^n$, where ΔW is the mass gain per unit area, k the oxidation rate constant, n the rate exponent, and t the exposure time.

Characterization of oxidation products was done on samples used for mass-gain determination. Phase identification of the oxide scale was performed by X-ray diffraction (XRD) using Co-K$_\alpha$ radiation. Surfaces and cross-sections of the oxidized specimens were studied by scanning electron microscopy (SEM). For avoiding discharges during SEM observations, the oxide scale was sputtered with a thin conductive gold layer. Once the surfaces were observed, a thick copper coating was deposited over the gold layer as a way for increasing contrast of the oxide scale in cross sectional views. Composition of the layer was qualitatively evaluated by energy dispersive X-ray microanalysis (EDX).

3. Results and discussion

Fig. 1 presents mass gain curves of W-2 V and W-4 V alloys. Apparently, no differences are noticed in the curves during the first 15 h of exposure for both alloys. Afterward, the mass gain of the W-4 V alloy becomes higher than that of the W-2 V alloy for exposures up to about 70 h. For longer times, mass gain curves run almost parallel in such a way that mass gain differences are kept almost constant from this moment to the end of the test. This suggests that mass gain differences are established during the transient stage in which almost linear kinetics are governing the oxidation, while the protective nature of the scale is
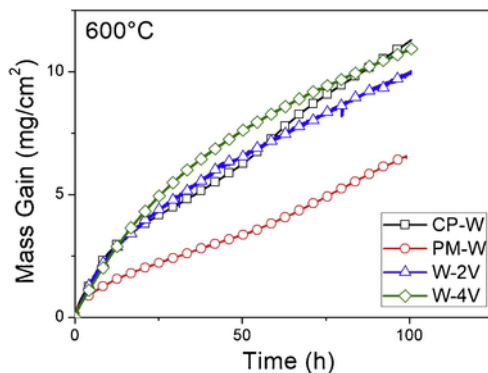
practically the same once the steady state is reached. This can be clearly seen by analyzing the evolution of the rate exponent (n) as the oxidation progresses. Two regimes can be distinguished: (1) The kinetics follow almost linear laws (n = 1.05 for W-2 V and n = 1.2 for the W-4 V) from the initial stages of oxidation. This stage extends up to about 10 h for the W-2 V alloy and 30 h for the W-4 V alloy. For longer oxidation times, the kinetics obey parabolic laws (n = 1.7 for W-2 V and 2 for W-4 V). Consequently, the higher mass gain measured in the W-4 V during the transient stage is clearly related to the shifting of linear kinetics towards longer times than in the case of the W-2 V alloy, i.e. 30 h versus 10 h. Nevertheless, the mass gains for both alloys are practically the same once the parabolic behaviour is attained, explaining the parallelism found in mass gain curves during the steady state.

For the potential use of W-V alloys in fusion applications, a comparison between the oxidation resistance of these alloys with that of pure ITER-reference tungsten grade, material selected for the manufacturing of the divertor armour of ITER, is required. Thus, mass gain curves of pure tungsten processed by two different routes, prepared by conventional metallurgy (CP-W) or powder metallurgy (PM), are also plotted in Fig. 1. It can be checked that the oxidation resistance of both W-V alloys are comparable with that of pure CP-W, although the occurrence of accelerated periods of mass gain due to breakaway events are suppressed with vanadium additions. However, the mass gain of both V-containing tungsten alloys is almost two times that of the PM-W, material also processed following powder metallurgy techniques. This suggests that tungsten with V additions has an oxidation resistance similar to CP-W when the alloys are prepared by powder metallurgy, but cannot enhance the improvement induced itself by the powder metallurgy processing.

Fig. 2 shows the XRD pattern of the W-2 V alloy oxidized at 600 °C during 100 h. XRD results evidence that the scale consists mostly of WO$_3$, with minor amounts of vanadium oxides (V$_2$O$_5$). Surface and cross sectional SEM observations provide relevant information about the structure of the scale and the distribution of V$_2$O$_5$ in the WO$_3$ scale. Fig. 3 presents the surface of the oxide scale formed over the two W-V alloys after 100 h of oxidation. The scale is similar for both alloys and it consists of an irregular distribution of long thin plates emerging from the continuous oxide layer. Since the kinetics obey parabolic laws, cracks observed in the surface are generated during cooling from the oxidation temperature, once the oxidation test was ended. In agreement with XRD measurements (see Fig. 2), the continuous layer corresponds to WO$_3$, while small peaks of V$_2$O$_5$ in the XRD pattern arise from thin plates. Atomic composition of these plates, measured by EDS microanalysis, is 69.2 ± 0.2 O, 29.2 ± 0.1% V and 0.9 ± 0.1 W. This stoichiometry agrees rather well with small peaks of V$_2$O$_5$ detected in XRD patterns (Fig. 3).

Cross sections of the oxidized alloys are presented in Fig. 4. Although the higher mass gain corresponds to the W-4 V alloy, the thickness of the oxide scale formed over the W-2 V alloy is slightly thicker than that established over the W-4 V alloy, 74 and 72 μm, respectively. This discrepancy can be explained by the different grade of densifica-

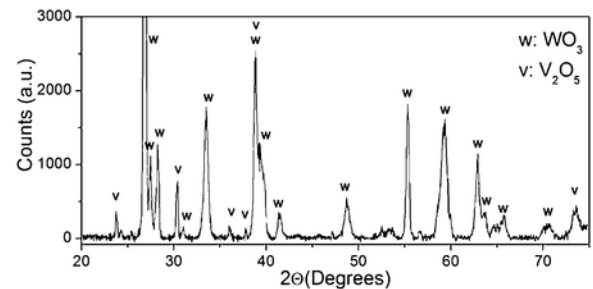**Fig. 1.** Mass gain curves for W-2 V and W-4 V alloys isothermally oxidized in dry air for 100 h at 600 °C. For reference, the curves of pure CP-W and PM-W are also plotted [15].

Fig. 2. XRD pattern of the scale formed on the W-2 V alloy after 100 h of exposure at 600 °C in dry air.
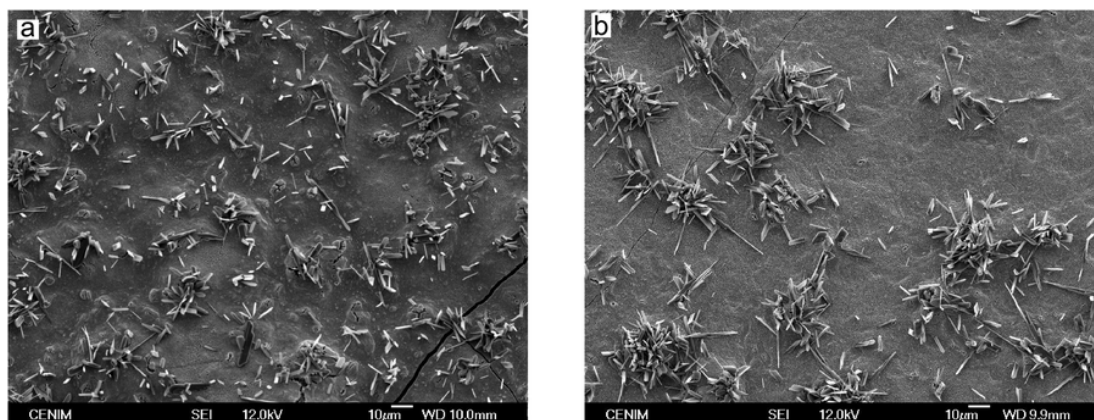
Fig. 3. Surface of the oxide scales developed after 100 h of exposure in dry air. (a) W-2 V alloy, (b) W-4 V alloy. Cracks observed in the images are generated during cooling from the oxidation temperature, not during oxidation tests.
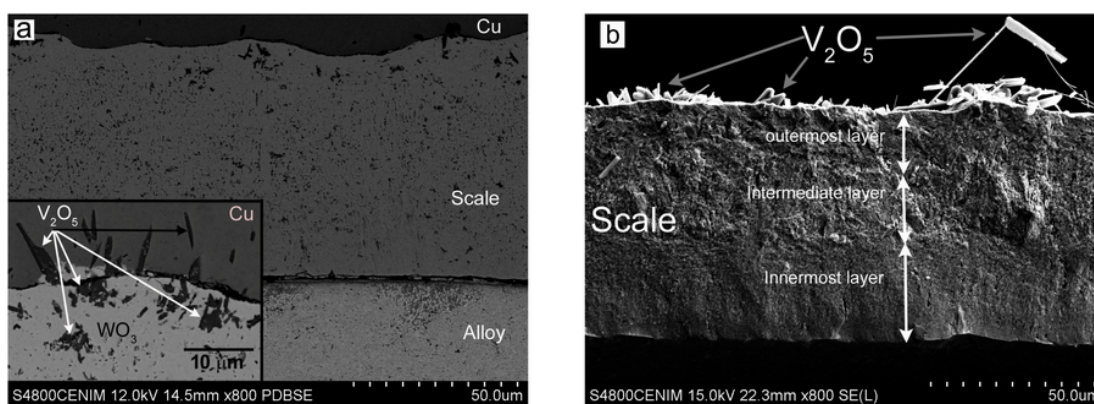

Fig. 4. Cross sectional views of the scales formed after 100 h of exposure in dry air. (a) W-2 V alloy (backscattered image), (b) W-4 V alloy. The scale was detached during cooling due to thermal stresses (secondary electron image). The inset shows a detail of V_2O_5 oxides at the outermost part of the oxide scale.

tion of the scale, as will be discussed later. The structure of the oxide layer is very similar and it can be divided into four regions: (a) Isolated outcrops of V-rich laths growing freely at the air/scale interface. (b) A relatively dense outermost layer of about 20–24 μm, consisting of a matrix of WO_3 (as deduced from XRD patterns) embedding particles of vanadium oxide (dark phase in backscattered images of Fig. 4). These particles belong to the V-rich laths found at the surface and they appear as a discontinuous phases because they grow in a different direction to that of the metallographic section, i.e. they do not usually emerge perpendicular to the original surface of the non-oxidized sample. (c) Intermediate porous layer of 35 μm for the W-2 V alloy and 20 μm for the W-4 V alloy, probably corresponding to $WO_{2.92}$ [13]. (d) The innermost layer, at the scale/alloy interface, is again relatively dense. The thickness was about 17 and 26 μm, for the W-2 V and W-4 V alloy, respectively.

Analysis of XRD data, surface and cross-sectional observations of the scale and mass gain curves provides information about the oxidation mechanism. During the initial stages of oxidation, kinetics are almost linear. This means that the oxide layer formed on the surface is not protective due to the development of a porous oxide layer which favors rapid inward oxygen ingress into the metallic substrate. Under these conditions, tungsten and vanadium can form their oxides. The scale will consist of a matrix of tungsten oxide embedding vanadium oxides. Nevertheless, as the oxide scale becomes thicker, the oxygen gradient through the scale tends to decrease gradually. Thus, the oxygen partial pressure can drop to the point at which no more vanadium oxides are formed at the scale/metal interface, being only oxidized the tungsten. Then, the oxidation behaviour resembles that described for

pure PM-W. In fact, mass gain curves become almost parallel for exposures longer than 65 h.

Cross sections reveal that the scale grows at the scale/metal interface due to rapid oxygen transport across the scale [13,15]. Consequently, no tungsten and vanadium should be available for the growth of new oxide at the surface of the scale. However, the structure of the outermost scale, consisting of V_2O_5 plates whose bases are embedded in a dense tungsten layer, implies simultaneous tungsten and vanadium transport from the alloy. In the case of pure tungsten the growth of the outermost part of the scale has been associated with outwards tungsten transport through the volatilization of $WO_{2.92}$ from the intermediate layer [13]. A similar transport mechanism might occur in the case of present W-xV alloys. It has been reported the low thermodynamic stability of vanadium oxides in contact with alloy in several W-V alloys exposed in the 900–1300 °C temperature range [11], causing dissociation of vanadium oxides. Thus, the development of long V-rich plates growing outwards at the air/scale interface could be explained assuming transport of vanadium from the alloy towards the scale/air interface through volatile species, i.e. volatile mixed tungsten-vanadium oxides.

The development of the triple layered structure in the scale can be explained as follows. Initially a non-protective porous oxide layer of $WO_{2.92}$ is formed, allowing the rapid ingress of oxygen into the alloy [13]. This porous layer corresponds to the intermediate layer observed in the cross section after 100 h of oxidation. The progressive decrease of the oxygen partial pressure across this layer results in the formation of volatile W-V oxides. These oxides leave outwards towards the air/scale interface. There, the oxygen pressure is higher and these oxides

can condensate as WO_3 and V_2O_5 oxides [13]. This would explain why outermost WO_3 layer grows outwards, embedding V_2O_5 laths during its growth, as observed in the outer part of the scale (see the inset of Fig. 4a). With time, this scale becomes dense, constituting an effective barrier for inward ingress of oxygen. This outermost scale is the responsible of the deceleration of kinetics from linear to parabolic (see mass gain curves in Fig. 1), since it fixes the content of oxygen at the interface between outermost and intermediate layers. Oxygen, however, is transported rapidly through the intermediate layer towards the interface with the substrate. In any case, the oxygen flow through the scale is slowed down considerably compared to that existing in the intermediate layer during the initial stages of oxidation. The vanadium content of the alloy also influences the oxidation behaviour of the alloys. Mass gain curves as well as cross sectional views of the scale clearly demonstrate that vanadium addition increases the oxidation rate during the initial stages of oxidation, probably induced by accelerated oxidation of vanadium. Therefore, the mass gain becomes higher as the vanadium content increases. However, a high V content also favours the sealing effect of V_2O_5 laths by blocking inward oxygen transport, turning the outermost WO_3 denser and protective. By this reason the thickness of the intermediate layer is thinner for the W-4 V alloy (see cross sections of the scales developed in W-2 V and W-4 V presented in Fig. 4).

4. Conclusions

From the present work the following conclusions can be drawn:

1 Vanadium addition has a negligible effect on the oxidation of pure tungsten.
2 The occurrence of periodical microcracking within the oxide scale, described for pure tungsten, is suppressed by vanadium additions, but the scale formed during the initial stage of oxidation is very porous.
3 Slowdown of oxidation kinetics is due to the formation of a continuous external WO_3 layer which acts as an effective barrier, reducing oxygen transport into the alloy.

Acknowledgments

References

[1] G. Federici, C. Bachmann, et al., Overview of the design approach and prioritization of R&D activities towards an EU DEMO, Fusion Eng. Des. 109–111 (2016) 1464–1474.
[2] D. Maisonnier, I. Cook, et al., The European power plant conceptual study, Fusion Eng. Des. 75–79 (2005) 1173–1179.
[3] Y. Ueda, K. Schmid, et al., Baseline high heat flux and plasma facing materials for fusion, Nucl. Fusion 57 (33) (2017) 092006.
[4] A. Malizia, L.A. Poggi, et al., A review of dangerous dust in fusion reactors: from its creation to its resuspension in case of LOCA and LOVA, Energies 8 (9) (2016), 578.
[5] R. Neu, J. Riesch, et al., Advanced tungsten materials for plasma-facing components of DEMO and fusion power plants, Fusion Eng. Des. 109–111 (2016) 1046–1052.
[6] T. Palacios, J.Y. Pastor, M.V. Aguirre, A. Martín, M.A. Monge, A. Muñoz, R. Pareja, Mechanical behavior of tungsten–vanadium–lanthana alloys as function of temperature, J. Nucl. Mater. 442 (2013) s214–s218.
[7] M.V. Aguirre, A. Martín, J.Y. Pastor, J. Llorca, M.A. Monge, R. Pareja, Mechanical properties of Y_2O_3-doped W-Ti alloys, J. Nucl. Mater. 404 (3) (2010) 203–209.
[8] T. Palacios, A. Jimenez, A. Muñoz, M.A. Monge, C. Ballesteros, J.Y. Pastor, Mechanical characterisation of tungsten-1 wt.% yttrium oxide as a function of temperature and atmosphere, J. Nucl. Mater. 454 (2014) 455–461.
[9] A. Muñoz, B. Savoini, E. Tejado, M.A. Monge, J.Y. Pastor, R. Pareja, Microstructural and mechanical characteristics of W–2Ti and W–1TiC processed by hot isostatic pressing, J. Nucl. Mater. 455 (1–3) (2014) 306–310.
[10] J. Stringer, The vanadium-oxygen system–a review, J. Less Common Met. 8 (1965) 1–14.
[11] I.Y. Lazareva, Y.I. Belov, E.M. Lazare, Kinetics and mechanism of oxidation of tungsten-vanadium alloys, Russ. Metall. 5 (1982) 172–174.
[12] A. Muñoz, M.A. Monge, B. Savoini, M.E. Rabanal, G. Garces, R. Pareja, La_2O_3-reinforced W and W–V alloys produced by hot isostatic pressing, J. Nucl. Mater. 417 (1-3) (2011) 508–511.
[13] S.C. Cifuentes, M.A. Monge, P. Pérez, On the oxidation mechanism of pure tungsten in the temperature range 600-800°C, Corros. Sci. 7 (2012) 114–121.
[14] A. Muñoz, M.A. Monge, B. Savoini, R. Pareja, A. Radulescu, SANS characterization of particle dispersions in W-Ti and W-V alloys, Int. J. Refract. Metals Hard Mater. 61 (2016) 173–178.
[15] S.C. Cifuentes, A. Muñoz, M.A. Monge, P. Pérez, Influence of processing route and yttria additions on the oxidation behavior of tungsten, J. Nucl. Mater. 442 (2013) S214–S218.